Three-photon resonant atomic excitation in spatially incoherent laser beams

Victor Peet and Sergei Shchemeljov
Institute of Physics, University of Tartu, Riia 142, Tartu 51014, Estonia
(Received 17 June 2003; published 22 October 2003)

Two-color excitation by spatially coherent and incoherent laser beams has been used to study three-photon-resonant excitation and subsequent ionization of xenon in conditions, when internally generated sum-frequency field plays an important role in excitation of atomic resonances through interfering one-photon excitation pathway. We show that the incoherence in one of the pumping fields reduces the efficiency of generated sum-frequency field, and thus suppresses the interference between the three- and the one-photon excitation channels. The degree of suppression is controlled by varying the crossing angle between coherent and incoherent laser beams. We show that ionization profiles can be analyzed on the basis of the well-studied interference of one- and three-photon transition amplitudes, but with pumping field decomposed into multiple small-scale uncorrelated domains where coherent process of four-wave mixing occurs. The gain length for a coherent process in these domains depends on the coherence degree and excitation geometry. It gives a possibility of controlling the contribution of coherent processes to the excitation of multiphoton resonances.

DOI: 10.1103/PhysRevA.68.043411 PACS number(s): 32.80.Rm, 42.65.Ky, 42.50.Ar

I. INTRODUCTION

Resonance-enhanced multiphoton ionization (REMPI) of atomic and molecular gases is a well-studied subject. An interesting REMPI phenomenon, also well studied, is that three-photon excitation profiles for a dipole-allowed transition may become completely suppressed [1–6] or shifted [7–11] from resonance position. These effects result from an internally generated sum-frequency field. For a certain threshold product of number density and oscillator strength, a sum-frequency field is generated under three-photon resonance pumping. This field becomes an important source of additional coherent excitation of atomic transitions. The overall excitation profile near the resonance results from a complicated interplay between interfering three- and one-photon excitation pathways [3,4,8–12]. At an elevated gas pressure, destructive interference of these coherent processes is able to suppress completely resonance excitation when no ionization peak is registered in REMPI spectra at the location of atomic resonance. For intense atomic resonances of xenon and krypton the cancellation effect may start to develop at a pressure as low as 10^{-2}–10^{-3} mbar [4]. This cancellation persists also when two different excitation wavelengths are used to drive the atomic transition [13].

In early experimental and theoretical studies, the cancellation effect was thought to be avoided with the use of counterpropagating laser beams when the resonance peak reappeared in the REMPI spectra [1–6]. However, such ''restored'' resonance was later found to have large pressure-dependent blue shift [7]. Again, this shift was explained as due to the internally generated sum-frequency field [8–12]. In any multibeam excitation geometry, a sum-frequency field evolves in amplitude and phase to suppress completely three-photon resonance excitation through a self-adjusted process of destructive interference everywhere except for a region on the blue wing of the atomic line. In this region interference becomes constructive and an intense ionization peak appears in the REMPI spectra. For unfocused beams this peak (or cooperative line) has the shape and amplitude identical to the pressure-broadened atomic line [8–11]. The location of the peak in the REMPI spectra is closely associated with the point where the real part of the phase mismatch between the pumping field(s) and generated sum-frequency field vanishes [14].

Multiphoton excitation and subsequent ionization of excited gas atoms could be a very effective method to study modifications of atomic resonant lines in conditions of extreme trapping of resonance radiation [7]. These transitions involve ground atomic state and the absorption of resonant photons is very strong. It makes the medium opaque for one-photon absorption or emission spectroscopy. To avoid opacity, the same dipole-allowed transitions can be driven by a three-photon excitation at a frequency where the medium is transparent. However, for such lines with large oscillator strength the cancellation effect is easily established and it suppresses multiphoton resonance excitation starting from relatively low gas pressure. With the use of counterpropagating beams an excitation profile can be registered but it is a shifted cooperative line produced in an essential manner due to the sum-frequency field, but not a ''real'' atomic peak.

Sum-frequency generation can be suppressed with the use of circularly polarized laser light. In this case, however, the number of atomic levels accessible for multiphoton excitation becomes limited by a selection rule for the magnetic quantum number $\Delta M = \pm K$, where K is the number of photons involved in multiphoton absorption. In rare gases the resonance transitions from the ground state to the lowest ns, ns', and nd excited states have $\Delta J = 1$, hence the three-photon excitation of these states by circularly polarized light is forbidden.

There is another way to diminish the influence of the sum-frequency field on resonance excitation. Evolution of this field in amplitude and phase along the propagation axis proceeds by a coherent transfer of energy from the pumping field(s). This process should be degraded essentially if any of the pumping fields has a poor wave-front coherence. For a coherent laser beam, regular coherence relations persist over an entire excitation region. By contrast, in a quasimonochro-

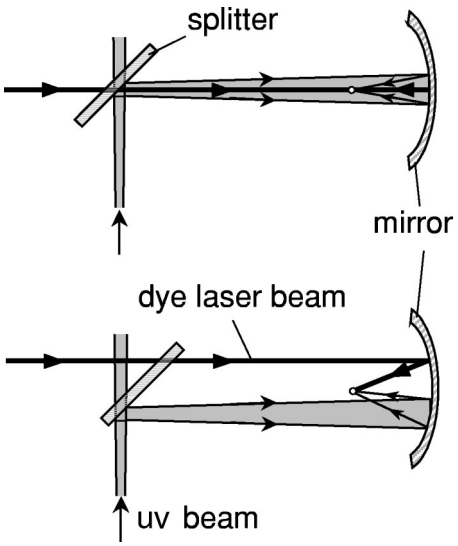

FIG. 1. Geometry of the two-color excitation: top, collinear excitation; bottom, noncollinear excitation.

matic light with low degree of spatial coherence, the field components are correlated in a transverse plane within some small-scale regions, but not over entire cross section of the beam. These local correlations decay after passing some propagation distance described in terms of longitudinal spatial coherence [15–19]. With the use of spatially incoherent laser light, the excitation volume is thus decomposed in both transverse and longitudinal directions into multiple small-scale regions, where some degree of coherence persists, but these coherent domains are mutually uncorrelated. Obviously, the effective length of coherent interaction is reduced in incoherent beams to the mean size of coherent domains. Coherent light beams were the basis of previous experimental and theoretical studies on the interplay between the one- and the three-photon excitation processes. In the present paper, we report experimental observations and analysis of these effects for the case of a mixed two-beam excitation by spatially coherent and incoherent laser beams.

II. EXPERIMENT

In REMPI experiments, the three-photon excitation and subsequent ionization of gas atoms was measured in a static gas cell. The cell was made of stainless steel and contained xenon at a pressure up to 200 mbar. Photoelectrons resulting from multiphoton ionization process were monitored with a wire collector biased at $+20$ V. Ionization signals were amplified, digitized, and stored in a computer.

Two laser sources were used in the two-color experiments. The first source was a tunable dye laser operated in either 443–450 nm (Coumarin 120 dye) or 555–565 nm (Rhodamine N dye) spectral ranges. The laser pulses had energies of 1–2 mJ, a pulse duration of 8–10 ns, and spectral width of about 10 pm full width at half maximum (FWHM). Dye laser was pumped by a XeCl excimer laser. The excimer laser served additionally as a source of uv radiation ($\lambda = 308$ nm) synchronized with pulses of the dye laser. For this purpose, a portion of XeCl laser output was taken from the laser beam by a small mirror and directed to the gas cell.

Figure 1 shows two principal excitation geometries used in experiments. Dye and uv laser beams were made copropagating with the aid of a quartz splitter. The splitter had a small wedge angle and reflected about 4% of the uv pulse from every surface. One of these reflected uv beams was blocked and the second, with typical energy of 40–60 μJ, was directed to the gas cell. In the collinear excitation mode, both the uv and the dye laser beams propagated along the same axis. These beams passed through the windows of the gas cell and were focused back into the cell by an on-axis spherical mirror of (focal length $f=30$ mm. The use of the mirror allowed us to avoid chromatic aberrations. The same optical arrangement was used in experiments with crossed beams. In this case, however, some distance between the beam axes was introduced and both beams were made propagating in parallel. Focused by the mirror, beams crossed at the focal region. In this noncollinear excitation mode the aperture of the cell windows allowed us to get the crossing angle up to 20°.

Divergence of the dye laser beam (full angle 2θ) was 0.5 mrad and exceeded the diffraction limit by 1.5–2 times only. It means a high degree of the beam spatial coherence. It was checked with the use of a prism interferometer [20]. The initial beam was split into two sub-beams and one of these sub-beams was then rotated in its own plane by 180°. Being superimposed, sub-beams produced an interference pattern which reflected mutual correlations of different parts of the wave front. The experiments have shown very good visibility of interference fringes, and thus a high degree of spatial coherence over the whole cross section of the dye laser beam.

Divergence of the uv beam from the XeCl laser was 2–2.5 mrad full angle and exceeded the diffraction limit by about two orders of magnitude. Such a beam had low degree of spatial coherence and contained multiple wave-front irregularities with a characteristic lateral correlation given by the correlation radius $r_c \simeq \lambda/(2\theta) \sim 0.1$ mm.

Different degree of spatial coherence for the dye and the uv beams resulted in their essentially different focusability. Figure 2 shows focal spots of the beams measured by a charge-coupled device camera in the focal region of a quartz lens. Because of chromatic aberration, the minimum size of focal spots corresponded to slightly different focal distances. The size of spots was measured for different lenses having focal length from 450 mm to 100 mm and the results were extrapolated to the focal length $f=30$ mm of the mirror. Such an extrapolation gave the size of about 10 μm and about 70 μm for the dye and the uv beam, respectively. Simple estimate of the focal spot diameter $2w_0$ for incoherent beams $2w_0 \simeq (2\theta)f$ gives 60–75 μm in good agreement with experimental finding. The confocal parameter b of the focused dye laser beam was about 0.3 mm. For the uv beam, an effective length b^* of the focal region can be estimated as $b^* \sim 2w_0/\theta_0 \simeq 0.4$ mm, where $\theta_0 = D/2f$ is the focusing angle, and $D \simeq 10$ mm is the size of the uv beam on the mirror. Taking into account the losses on optical elements, the light intensity in the focal volume was of about 5×10^7 W/cm^2 for the uv pulse of 50 μJ and about 5×10^{10} W/cm^2 for the dye laser pulse of 1 mJ.

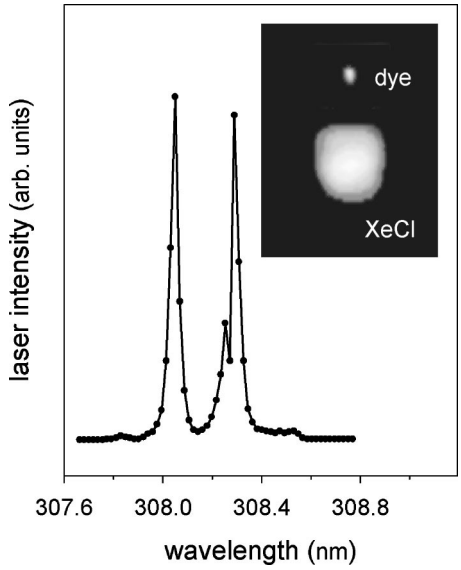

FIG. 2. XeCl lasing spectrum and focal spots of the used dye and XeCl laser beams.

According to the Van Citter-Zernike theorem [21], the ratio of the correlation radius r_c to the beam size remains unchanged under propagation. It means that in tightly focused incoherent beams the wave-front correlations can be squeezed in transverse directions to the size of a few wavelengths. These lateral local correlations decay after passing some coherence distance along the propagation axis. The length of such correlated propagation is described by the longitudinal spatial coherence function [15–19]. For a focusing angle $2\theta_0 = D/f$, the characteristic size of transverse d and longitudinal Δz correlations can be estimated as $d = 2r_c \simeq 2\lambda/(2\theta_0) \simeq 2\ \mu$m and $\Delta z \simeq 4\lambda/(2\theta_0)^2 \simeq 10\ \mu$m. Thus, the overall excitation volume of the uv beam can be considered as a set of multiple mutually uncorrelated spatial regions or coherent domains, where some degree of correlation is maintained. Within these domains, the field components may have all possible propagation directions within a cone with a characteristic angular spread of θ_0. Note that the correlation of field components increases the local light intensity and it facilitates excitation and ionization of gas atoms in corresponding regions. The pattern of coherent domains behaves like a transient speckled field, where correlation within a domain (or a transient speckle) is maintained during some time $t \sim \tau_c$, where τ_c is the temporal coherence time.

Figure 2 shows the lasing spectrum of the used XeCl laser. This spectrum was measured with a 1-m double monochromator operated in the third order of a grating 1200 lines/mm. Two intense lines in the spectrum correspond to vibronic transitions $0 \rightarrow 1$ and $0 \rightarrow 2$ of the XeCl molecules [22,23]. Two other lasing transitions $0 \rightarrow 0$ and $0 \rightarrow 3$ are much weaker. Main laser lines are separated by 0.24 nm or 25 cm^{-1} and have the width of about 40 pm FWHM. The dip in one emission line is due to absorption by OH radicals [24]. The overall width of the lasing spectrum is about 30 cm^{-1} and it corresponds to the coherence time of $\tau_c \sim 10^{-12}$ s and the temporal coherence length $l_c \sim 0.1$ mm.

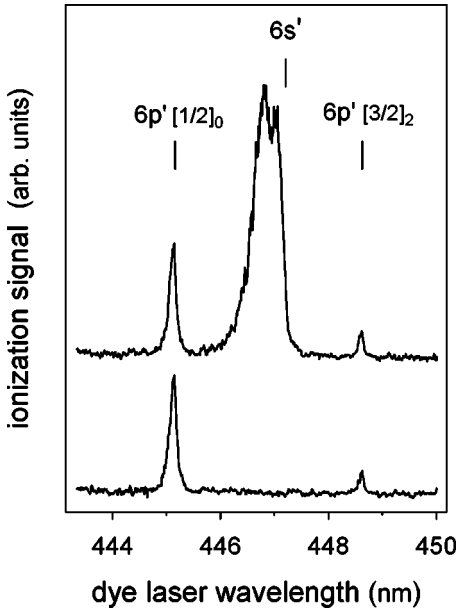

FIG. 3. Wavelength scans of ionization signal near 447 nm: bottom, one-color excitation by dye laser beam; top, two-color excitation with uv beam added. Collinear excitation; xenon pressure 50 mbar.

Note that in the focal region $\Delta z \ll l_c$.

The two-color excitation and subsequent ionization of the target gas occurs in the focal region of the overlapped dye laser and uv beams. The presence of small-scale transient domains in the uv field restricts the distance of coherent interaction of both beams to the mean size of these domains. The length of coherent interaction depends on the crossing angle since uv domains are extended along the uv beam axis. This length is maximum for copropagating beams and it is minimum for beams crossed at a right angle. In our experiments, the beams had crossing angles of up to 20° and the overall excitation volume, given by the focal volume of the dye laser beam, contained an order of 10^3 domains from the uv field.

III. RESULTS AND DISCUSSION

The lowest states of xenon accessible for three-photon excitation by linearly polarized light are the $6s$ and the $6s'$ states having excitation energies of 8.437 eV and 9.570 eV, respectively. Since one laser source ($L2$) is fixed near 308 nm, the corresponding three-photon transitions $2\omega_{L1} + \omega_{L2}$ should be induced at the dye laser wavelength near 447 nm for the $6s'$ state and near 562 nm for the $6s$ state. Excited $6s$ atoms are ionized through the absorption of either one uv or two dye laser photons. Excited $6s'$ atoms are ionized by the absorption of one photon from uv or dye laser beams. Figures 3 and 4 show the REMPI spectra measured in corresponding spectral regions. The dye laser beam alone produced several ionization peaks due to the four-photon excitation of $6p'$ (Fig. 3) or the five-photon excitation of $6d$ states of xenon (Fig. 4). With a uv beam added, an intense ionization band appeared in spectra. Note that the intensity of the uv light in the focal volume was by three orders of

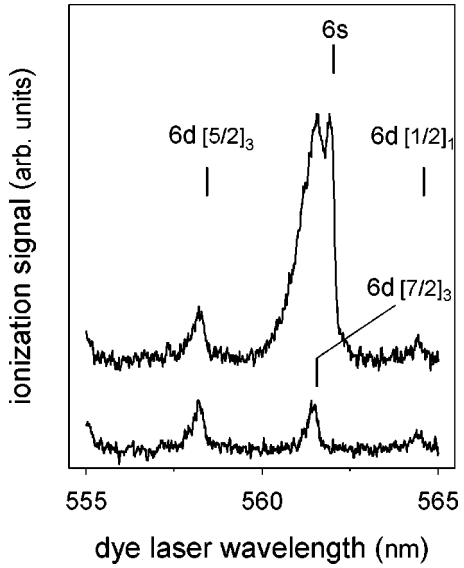

FIG. 4. Wavelength scans of ionization signal near 560 nm: bottom, one-color excitation by dye laser beam; top, two-color excitation with uv beam added. Collinear excitation; xenon pressure 50 mbar.

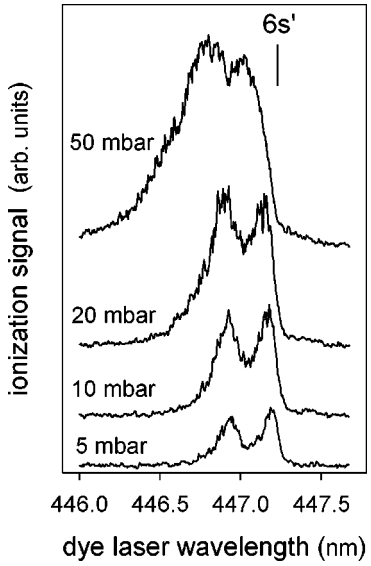

FIG. 5. Evolution of the ionization band with pressure in collinear beams.

magnitude lower than the intensity of the dye laser beam. The ionization band had a distinct doublet structure with peaks separated by 0.25 nm near 447 nm and by 0.4 nm near 562 nm. In both cases this spectral distance corresponds to 12.5 cm^{-1} and this is exactly one half of the 25 cm^{-1} separation of the peaks in the XeCl lasing spectrum (Fig. 2). Thus, the ionization bands are due to the three-photon resonant absorption $2\omega_{L1}+\omega_{L2}$ as expected. The location of the three-photon $6s'$ and $6s$ resonances marked in Figs. 3 and 4 corresponds to the line $\lambda=308$ nm in the XeCl laser spectrum.

For the $6s$ resonance, the ionization band overlaps the peak of the five-photon $6d[7/2]_3$ resonance (Fig. 4). This peak is produced by the dye laser beam alone and it leads to some distortions of the ionization band registered under two-beam excitation. Therefore, a detailed study of three-photon resonance excitation was carried out for the $6s'$ resonance, where the corresponding spectral region is free of additional ionization features. Figure 5 shows evolution of ionization profiles with pressure in collinear excitation geometry. At low gas density, the ionization profile has two well-separated peaks which correspond to two emission lines in the uv beam. With an increased pressure, these peaks are broadened rapidly and overlap. Above 50 mbar the doublet structure of the band becomes unresolved and the ionization profile is registered as a single broad band. Broadening of profile components is followed by a distinct shift of the peaks from the resonance position toward a shorter wavelength. Such an evolution of ionization profiles with pressure is a distinct indication for a well-known excitation process where internally generated sum-frequency field dominates the resonant excitation [8–11]. Note that for collinear two-color excitation by *coherent* beams no on- and off-resonance excitation is expected in a dense gas [9–11,13]. In this case, the resonance peak is canceled and no phase-matched sum-frequency field is produced in the vicinity of the resonance.

Figure 6 shows pressure-dependent ionization profiles for noncollinear excitation by beams angled by 18°. For pressures below 20 mbar no measurable changes in location and width of the peaks could be detected. The minimum width of the peaks was 0.1 nm which corresponds to 10 cm^{-1} in a two-photon scale. Compared with the width of 4 cm^{-1} for the uv laser lines, a significant contribution to the width of ionization peaks from the ac Stark effect can be stated. For the three-photon pumping of the lowest $6s$ resonance of xenon, the ac Stark shift constant of 0.44 $cm^{-1}\,GW^{-1}\,cm^2$ was reported in Ref. [25]. For the case here, it means the magnitude of the ac Stark shift for the $6s$ resonance of about 20 cm^{-1}. For the $6s'$ resonance some similar ac Stark shift constant is expected. Thus, the broadening of the ionization

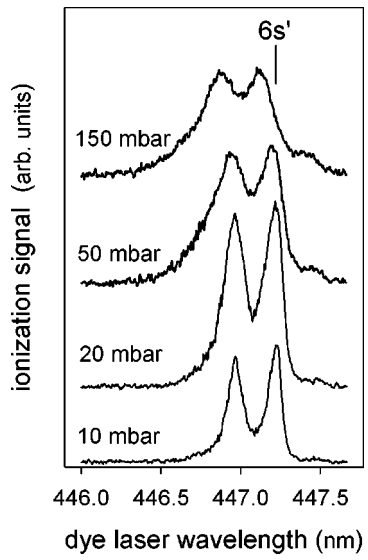

FIG. 6. Evolution of the ionization band with pressure in crossed beams. Crossing angle $\alpha=18°$.

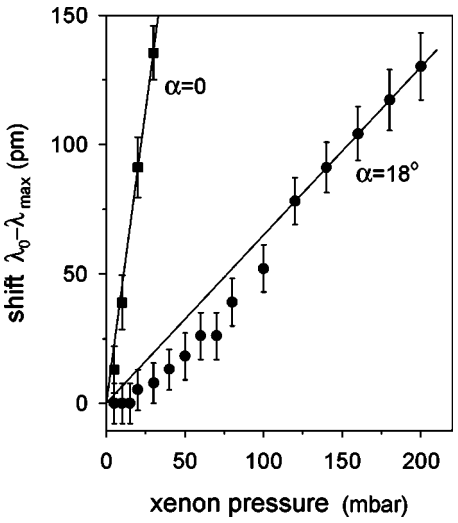

FIG. 7. Pressure-induced shift of the ionization peaks.

peak should be of the order of 10 cm^{-1} in agreement with the experimental observations. This broadening can be reduced through a decrease of the dye laser pulse energy. To keep the overall excitation probability, this decrease should be followed by an increase of the uv pulse energy. In our case, however, we had to keep the uv light intensity low since the intense uv light produced a strong parasitic ionization in the gas cell.

Above 20 mbar, discernible broadening and blue shift of ionization peaks become evident. This shift and broadening were however much smaller than in the collinear case and a distinct doublet structure of the band could be detected at any gas pressure. Again, these transformations together with the sensitivity to the crossing angle are distinct indications of the excitation process where the sum-frequency field plays an important role.

Figure 7 shows plots of the shift with pressure of ionization peaks. For collinear beams, the shift and width of the ionization band were very sensitive to the shape of the uv beam and mutual arrangement of uv and dye laser beams. The shift was linear with pressure and in different series of measurements a slope of 3.5-8 nm/bar was obtained. The dependence shown in Fig. 7 has the slope of 4.5 nm/bar. For noncollinear beams with a relatively large crossing angle, the sensitivity to the beam shape and adjustment was much weaker. In this case, sharp ionization peaks were well-pronounced over the whole pressure range and the shift could be measured with good accuracy. For crossing angle $\alpha=18°$, the shift becomes linear with the slope of 0.65 nm/bar above 100 mbar, but distinct deviations from this linear dependence were observed for the lower pressure range. The same behavior was observed in all other series of measurements with different crossing angles.

We start the analysis of experimental findings from pressure dependences. The shift of ionization peaks is linear with pressure and has distinct dependence on the crossing angle. These observations exactly follow the well-known pattern of the three-photon-resonant excitation by crossed laser beams [8–11]. For two angled beams with angular frequencies ω_{L1} and ω_{L2} the frequency shift of the ionization profile from the resonance position is given by [9–11]

$$\Delta_c=\Delta_0\left[\frac{\lambda_{L1}+2\lambda_{L2}}{\lambda_{\mathrm{mix}}(1-\cos\alpha)}\right], \tag{1}$$

where $\Delta_0=\pi NF_{01}e^2/2m\omega_0$, $\lambda_{\mathrm{mix}}=2\pi c/(2\omega_{L1}+\omega_{L2})$, N is the gas density, F_{01} is the oscillator strength, and ω_0 is the resonance angular frequency. Parameter Δ_0 and the width Γ (FWHM) of the pressure-broadened atomic line are coupled by the relation $\Gamma=4.66\Delta_0$ [26]. For the $6s'$ resonance of xenon Γ/N and Δ_0/N are 3.2 cm^{-1}/bar and 0.7 cm^{-1}/bar, respectively. The shift Δ_c is minimum at $\alpha=\pi$ and is directly proportional to gas pressure. When crossing angle is decreased the shift Δ_c becomes very large and starting from some minimum angle θ_{min} the ionization signal is decreased rapidly. In high-pressure xenon θ_{min} is about 0.1 rad [11]. For $\alpha>\theta_{\mathrm{min}}$, the ionization peak has the appearance of pressure-broadened atomic line, i.e., it has the same amplitude and shape as the atomic line.

For a collinear two-color excitation $\alpha=0$ and no ionization is produced near the atomic resonance since the excitation pathway through the atomic resonance is canceled and no phase-matched sum-frequency field is generated near the resonance. It is a well-known observation in experiments on a collinear two-color resonant ionization in dense gases [9,13]. Note, however, that the laser sources in Refs. [9,13] had a high degree of spatial coherence as a common feature of the narrow-band excimer-pumped dye lasers. Such regular coherent beams maintain the collinearity condition $\alpha\simeq0$ over the whole interaction region. In our case, one of the interacting light fields has poor wave-front coherence and the excitation region is irregular with multiple coherent domains. The angular spectrum of an incoherent light field determines some range of different propagation directions of the field components and an essential local noncollinearity persists even for a collinear propagation of the coherent and incoherent beams. According to Eq. (1) the slope of 4.5 nm/bar for a collinear excitation (Fig. 7) corresponds to the crossing angle $\alpha\simeq9°$ which is very close to the focusing angle $\theta_0\simeq10°$ of the uv beam. For beams angled by $\alpha=18°$ the slope was 0.65 nm/bar (Fig. 7). Formally, such a slope corresponds to the crossing angle $\alpha\simeq24°$.

In order to simulate the excitation profiles, we used the concept of the cooperative line shift together with a simple geometrical consideration. The incoherent beam was considered as a set of small coherent domains having cylindrical symmetry and extended along the propagation axis z (Fig. 8). The angular spectrum of the incoherent field determines some range of crossing angles for the field components. All these components were assumed to have equal amplitudes with uniform distribution within a range of angles from zero to the maximum angle θ_0. In k space, such an approximation makes the wave vectors $\mathbf{k}_{L2}$ be distributed uniformly along all possible directions inside a cone with the half angle θ_0. The coherent wave enters as a regular Gaussian beam, but for small-scale domains the length of the coherent four-wave interaction Δz is much smaller than the confocal parameter b of the focused Gaussian beam. Besides, transient intensity

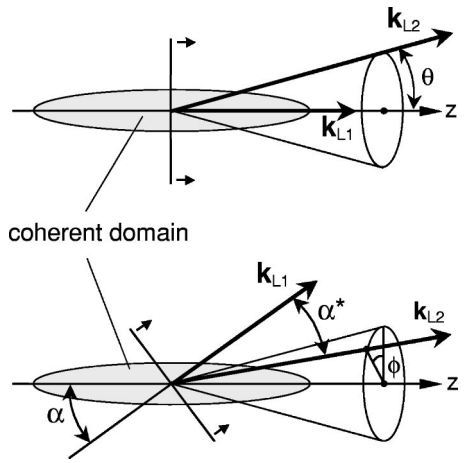

FIG. 8. Wave-vector diagram for interaction of coherent and incoherent light fields: top, collinear excitation; bottom, noncollinear excitation.

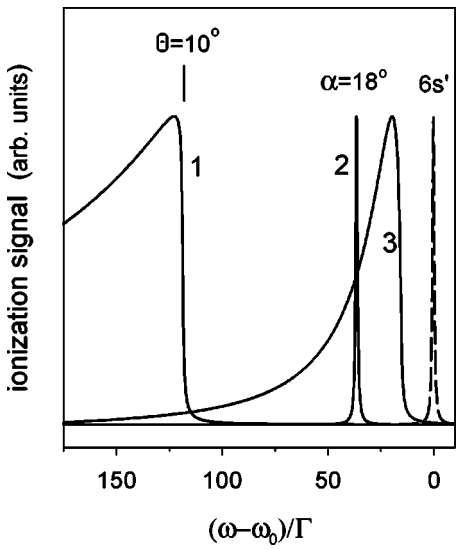

FIG. 9. Numerical simulation of near-resonance excitation profiles: 1, collinear excitation by coherent and incoherent beams; 2, Lorentzian profile for two coherent beams with crossing angle $\alpha = 18°$; 3, coherent and incoherent beams with crossing angle $\alpha = 18°$. The dashed line shows the resonance atomic line.

spikes in a multimode dye laser pulse have a duration of 10^{-10}–10^{-11} s and such intensity changes are slow in the time scale of $\Delta z/c$. Thus, within the uv domains one can neglect all changes (associated with either focusing or spiking) of the dye laser beam in amplitude and phase, and consider the coherent beam as a regular plain wave. In a collinear case, both the coherent and incoherent beams propagate along the same axis *z* but angular spreading of the field components results in some spreading of the crossing angle α between the wave vectors $\mathbf{k}_{L1}$ and $\mathbf{k}_{L2}$. Obviously, this range of angles is from 0 to θ_0. A similar situation is valid for crossed beams, where the crossing angle α^* between the wave vectors $\mathbf{k}_{L1}$ and $\mathbf{k}_{L2}$ is determined as

$$\cos\alpha^* = \cos\theta\cos\alpha + \sin\theta\sin\alpha\cos\phi, \qquad (2)$$

where ϕ is the azimuth angle (see Fig. 8). For $\alpha > \theta_0$, the angle α^* changes from $\alpha - \theta_0$ to $\alpha + \theta_0$.

Simple geometrical consideration shown in Fig. 8 allows one to reduce the excitation problem for incoherent light field(s) to the well-known problem of the interaction of *coherent* waves propagated in an absorbing medium. Again, for a pair of crossed plain waves the concept of the cooperative line shift predicts the excitation profile as a Lorentzian peak shifted to the blue side of the resonance position. The value of this shift is given by Eq. (1). For coherent beams the interaction geometry is characterized entirely by a given crossing angle α, whereas for incoherent field(s) an additional angular variable θ enters the excitation problem.

Every partial configuration of interacting waves produces a Lorentzian excitation profile, but instead of a single Lorentzian peak for coherent waves a more broad excitation profile is expected for incoherent fields because of the angular spreading. In this sense, the excitation problem for interaction of coherent and incoherent waves is very similar to the three-photon excitation by coherent Bessel beams [27–29]. For conical Bessel beams the three-photon excitation profile near the atomic resonance builds up as a superposition of multiple Lorentzians, where every individual Lorentzian corresponds to some spatial configuration of sub-beams from the fundamental light cone [29]. In the same manner, the excitation profile for interaction of coherent and incoherent waves builds up from multiple configurations of angled waves. This superposition includes all possible subscriptions of the wave vectors $\mathbf{k}_{L2}$ within the cone of the angular spreading. Every elementary profile in this superposition has the same appearance of the atomic line, i.e., all profiles are Lorentzians having equal amplitudes and widths Γ. This situation has been analyzed in detail in Ref. [29] and we have used here the same approach.

Figure 9 shows the excitation profiles calculated for the collinear and noncollinear interactions of coherent and incoherent beams. For the incoherent beam, the maximum spreading angle $\theta_0 = 10°$ was assumed. For collinear beams the angle θ_0 determines the red edge of the region (or the minimum value of available cooperative shift) where individual Lorentzians are located. This red edge is marked in Fig. 9. Note that the approach of equal Lorentzians is valid when $\alpha > \theta_{\min}$. Thus, the detuning Δ_c in calculations was limited by the range $\Delta_c < 200\Gamma$. For larger detunings the ionization signal is reduced rapidly (and, thus the approach of equal Lorentzians breaks down) since the medium becomes transparent for the sum-frequency light. In this case, a phase-matched vacuum uv (vuv) emission near $\lambda \simeq 129$ nm exits the excitation region. This weak low-coherent vuv light is confined within a range of angles $\theta < \theta_{\min}$.

Superposition of multiple Lorentzians in a collinear case produces the excitation profile peaked very close to the red edge of the region, where Lorentzians are spread. It agrees well with the experimental observations, where the excitation profile for a collinear geometry demonstrated a distinct evidence of noncollinearity with an effective crossing angle of 9°, which is very close to the experimental value $\theta_0 \simeq 10°$. The maximum of the calculated profile is located at $\Delta_c \simeq 125\Gamma$ which corresponds to about 400 cm^{-1}/bar. In

terms of the dye laser wavelength, such detuning corresponds to the pressure-induced shift of 4 nm/bar and it is in good agreement with experimental findings. Qualitatively, formation of the peak near the red edge can be understood as follows. First, for a uniform angular distribution of the field components the spectral density of the Lorentzian peaks is increased rapidly toward the resonance. Second, due to an axially symmetric excitation geometry, the Lorentzians for a given θ enter superposition with an annular weighting factor $\sin\theta$. Thus, the envelope of superimposed Lorentzians gains intensity toward the region of large θ and small detunings from the resonance.

Noncollinear excitation by two crossed *coherent* beams produces an excitation profile as a Lorentzian peak located on the blue side of the atomic resonance. This profile is shown in Fig. 9 for the crossing angle $\alpha=18°$, when the shift $\Delta_c \simeq 36\Gamma$. For crossed coherent and incoherent beams, the crossing angle between the field components becomes spread within some range and a variable angle α^* determines the excitation geometry instead of a fixed angle α (see Fig. 8). Again, every partial combination of the interacting waves produces a Lorentzian peak and these elementary Lorentzian profiles are spread within some spectral range. The crossing angle α^* is given by Eq. (2), where θ changes from 0 to θ_0 and ϕ changes from 0 to 2π. The overall excitation profile is given by an integral of the Lorentzian profiles over angles θ and ϕ. This excitation profile is shown in Fig. 9. Superposition of multiple Lorentzians produces an excitation profile which is peaked closer to the resonance than the Lorentzian profile for coherent beams. Again, it results from an increasing spectral density and weighting factors for elementary Lorentzians toward the region of the maximum crossing angles α^*, and thus the minimum detunings from the resonance. The peak of the calculated profile is located at $\Delta_c \simeq 20\Gamma$ which corresponds to the pressure-induced shift of 64 cm^{-1}/bar or 0.64 nm/bar in terms of the dye laser wavelength. This value is in very good agreement with the shift of 0.65 nm/bar observed in experiment. Note distinct similarity of the ionization profile 3 in Fig. 9 and the ionization profiles for coherent Bessel beams [29] calculated with the same approach of multiple elementary Lorentzian profiles distributed near the atomic resonance.

The angular spreading of the field components in incoherent light field is responsible for a red shift of the ionization profiles with respect to the location of this peak in coherent beams. This difference is especially pronounced at small crossing angles, when the peak for a collinear geometry has a large shift. For interaction of the coherent and incoherent beams, the shift is smaller because of a significant local noncollinearity. The shift of the ionization peak in a collinear case corresponds approximately to the maximum angle of spreading of the field components in the incoherent beam.

The sum-frequency field dominates the off-resonance excitation in an absorbing medium. Our evaluation of the excitation profiles was based on a simple geometrical consideration together with the phase-matching requirements for the generated sum-frequency field, but did not include the length of the coherent interaction. This gain length accounts for intensity of the ionization peaks but not for the shape of the excitation profiles. The length of the coherent interaction, however, becomes a crucial factor for the on-resonance excitation, when the interference of the three- and the one-photon pathways determines resonance excitation. The evolution of the interfering sum-frequency field requires a certain (concentration dependent) propagation distance into the excitation zone. The drop in signal of the on-resonance excitation begins when the absorption length for the sum-frequency field becomes comparable with the length of the coherent interaction [4]. If this distance is too short for an evolution of the sum-frequency field in amplitude and phase, a complete cancellation is not established and the fundamental photons drive the three-photon excitation of the atomic resonance. For incoherent light fields, the length of a coherent interaction is determined by the mean size of coherent domains. Since domains are extended along the propagation axis, this length is reduced rapidly when crossing angle between the coherent and incoherent beams is increased (see Fig. 8). Considering the coherent domains as ellipsoids with axes d and Δz, the length L of the interaction as a function of the crossing angle α can be written as

$$L = \frac{d\Delta z}{\sqrt{\Delta z^2 \sin^2\alpha + d^2\cos^2\alpha}}. \tag{3}$$

For $\alpha=90°$ the length $L=d$ is minimum and can be as short as a few wavelengths. For such extremely short gain length the contribution of the sum-frequency field to the transition amplitude should be diminished significantly.

An incomplete cancellation of the atomic excitation is believed to be responsible for the observed deviations of the pressure-induced shift of the ionization peaks from a linear dependence (Fig. 7). In all experiments with angled beams, the shift becomes linear at an elevated gas pressure, but distinct deviations from this linear dependence occurred within a low-pressure region, where the peaks always had a smaller shift. An explanation of these observations is that the ionization signal at a low pressure contains a significant contribution from the uncanceled atomic resonance. At a low gas pressure, no cancellation occurs and a peak of the resonance excitation is registered. With an increased pressure, a sum-frequency field starts to develop. This field suppresses progressively the resonance excitation and increases the excitation on the blue wing of the atomic line. The resonance peak is very narrow (about 30 pm/bar in terms of the dye laser wavelength), therefore both the on- and off-resonance components are registered together as a single peak with small apparent shift. Further increase of pressure leads to a complete cancellation of the atomic resonance and the ionization profile becomes entirely due to the sum-frequency field. Without contribution from the unshifted atomic peak, the dependence of the pressure-induced shift becomes linear. Experiments have shown that a reduced apparent shift, and thus some contribution to the ionization profile from the uncanceled atomic peak, can be traced up to a pressure of about 100 mbar for the crossing angle $\alpha=18°$. With an increased α, the length of the coherent interaction is reduced rapidly and achieves a minimum at $\alpha=90°$. Thus, with an appropriate spectral resolution, the use of crossed coherent and inco-

herent beams may give a reliable possibility to detect the atomic resonance lines free of the interfering coherent effects.

IV. CONCLUSION

Three-photon resonant excitation and subsequent ionization in dense gases proceeds in conditions where generated sum-frequency field plays a crucial role in the on- and off-resonance excitation processes. The evolution of this sum-frequency field in a four-wave mixing process requires certain coherence relations for the driving fields. If at least one of these fields has low degree of the spatial coherence, a coherent four-wave interaction is maintained within small-scale mutually uncorrelated domains. The length of the coherent interaction within these domains depends on the coherent properties of the pumping field and excitation geometry. It gives a possibility of controlling the role and influence of the sum-frequency field in excitation processes.

Three-photon excitation of xenon atomic resonances by coherent and incoherent laser beams has shown distinct indications for the role of the sum-frequency field in the excitation processes. In a dense gas, this field is responsible for the appearance of intense ionization peaks on the blue wing of atomic resonance. The shape and pressure-induced shift of these peaks follow the known pattern of the resonance-enhanced multiphoton excitation and ionization in crossed laser beams. However, with the use of an incoherent light several specific effects have been observed. For excitation by copropagating coherent beams no near-resonance ionization signal is expected. By contrast, intense ionization profiles were detected with incoherent light in any excitation geometry. The shift of the ionization peaks from the atomic resonance for an incoherent light always was smaller than the shift of the corresponding peak in a coherent excitation mode. These effects have been explained on the basis of a simple geometrical consideration, where the incoherent light field enters the excitation problem as a set of multiple plain waves variously displaced within some range of angles. This angular spreading of the field components supports a local noncollinearity of the four-wave interaction in any excitation geometry. Based on this approach, a numerical evaluation of the off-resonance excitation profiles has been carried out and good agreement with experimental observation has been obtained.

A limited range of the coherent interaction in incoherent light beams may serve as a tool for diminishing the influence of the coherent processes on the excitation of atomic resonances in a dense gas. In experiments with angled coherent and incoherent beams, an indication of the presence of an uncanceled atomic resonance peak has been observed for a pressure range of several tens of millibars. In crossed beams it is quite easy to reduce the length of the coherent interaction to a few wavelengths, when the gain length becomes too short for evolution of the interfering sum-frequency field. It gives a possibility to avoid a complete suppression of the on-resonance excitation caused by destructive interference of the three- and the one-photon excitation pathways.

ACKNOWLEDGMENT

This work was supported by the Estonian Science Foundation under Grant No. 5030.

[1] J.C. Miller, R.N. Compton, M.G. Payne, and W.R. Garrett, Phys. Rev. Lett. **45**, 114 (1980).
[2] J.C. Miller and R.N. Compton, Phys. Rev. A **25**, 2056 (1982).
[3] M.G. Payne and W.R. Garrett, Phys. Rev. A **26**, 356 (1982).
[4] M.G. Payne and W.R. Garrett, Phys. Rev. A **28**, 3409 (1983).
[5] D.J. Jackson, J.J. Wynne, and P.H. Kes, Phys. Rev. A **28**, 781 (1983).
[6] M.G. Payne, W.R. Garrett, and W.R. Ferrell, Phys. Rev. A **34**, 1143 (1986).
[7] W.R. Ferrell, M.G. Payne, and W.R. Garrett, Phys. Rev. A **36**, 81 (1987).
[8] R. Friedberg, S.R. Hartmann, and J.T. Manassah, J. Phys. B **22**, 2211 (1989).
[9] W.R. Garrett, R.C. Hart, J.E. Wray, I. Datskou, and M.G. Payne, Phys. Rev. Lett. **64**, 1717 (1990).
[10] M.G. Payne and W.R. Garrett, Phys. Rev. A **42**, 1434 (1990).
[11] M.G. Payne, W.R. Garrett, R.C. Hart, and I. Datskou, Phys. Rev. A **42**, 2756 (1990).
[12] M.G. Payne, J.C. Miller, R.C. Hart, and W.R. Garrett, Phys. Rev. A **44**, 7684 (1991).
[13] W.R. Garrett, S.D. Henderson, and M.G. Payne, Phys. Rev. A **34**, 3463 (1986).
[14] W.R. Garrett, Y. Zhu, L. Deng, and M.G. Payne, Opt. Commun. **128**, 66 (1996).
[15] C.W. McCutchen, J. Opt. Soc. Am. **56**, 727 (1966).
[16] J.E. Biegen, Opt. Lett. **19**, 1690 (1994).
[17] J. Rosen and A. Yariv, Opt. Commun. **117**, 8 (1995).
[18] J. Rosen and A. Yariv, J. Opt. Soc. Am. A **13**, 2091 (1996).
[19] J. Rosen and M. Takeda, Appl. Opt. **39**, 4107 (2000).
[20] M.V. Murty, J. Opt. Soc. Am. **54**, 1187 (1964).
[21] L. Mandel and E. Wolf, *Optical Coherence and Quantum Optics*, 1st ed. (Cambridge University, Cambridge, UK, 1995).
[22] J. Tellinghuisen, J.M. Hoffmann, G.C. Tisone, and A.K. Hays, J. Chem. Phys. **64**, 2484 (1976).
[23] A. Sur, A.K. Hui, and J. Tellinghuisen, J. Mol. Spectrosc. **74**, 465 (1979).
[24] E.B. Berik, A.A. Vill, V.A. Davidenko, V.T. Mihkelsoo, and S.A. Tsarenko, in *Proceedings of International Conference Lasers-82, New Orleans, USA*, edited by R.C. Powell (STS Press, McLean, 1983), p. 365.
[25] P. Kruit, J. Kimman, H.G. Muller, and M.J. Van der Wiel, J. Phys. B **16**, 937 (1983).
[26] P.R. Berman and W.E. Lamb, Phys. Rev. **187**, 221 (1969).
[27] W.R. Garrett and V.E. Peet, Phys. Rev. A **61**, 063804 (2000).
[28] V.E. Peet, W.R. Garrett, and S.V. Shchemeljov, Phys. Rev. A **63**, 023804 (2001).
[29] V.E. Peet and S.V. Shchemeljov, Phys. Rev. A **67**, 013801 (2003).